CHEMICAL
PHYSICS
LETTERS

IncDFT: Improving the efficiency of density functional theory using some old tricks

Shawn T. Brown [*],[1], Jing Kong

Q-Chem, Inc., 5001 Baum Boulevard, Suite 690, Pittsburgh, PA 15213, USA

Abstract

Presented in this Letter is the IncDFT method, which utilizes the difference density to compute the DFT numerical integration, and is formulated so that the problem of using non-linear functionals is circumvented and proper mathematic consistency is maintained. As convergence is approached, an increasing amount of values associated with the numerical quadrature can be neglected. The IncDFT method has been implemented with a variable threshold in Q-Chem 2.1, and yields up to 45% savings in the time needed for the integration procedure with negligible loss in accuracy.
© 2005 Elsevier B.V. All rights reserved.

1. Introduction

In the landscape of modern quantum chemical methods, Density Functional Theory (DFT) stands tall as the premier method for computing molecular energies and properties. There are several reasons why the method is so widely used over traditional wavefunction based approaches, with the main reason being its applicability to a wider range of molecular systems. Quantum chemists primarily use the Kohn–Sham formulation of the DFT (KS-DFT) which allows the theory to be derived in a way that allows for easy integration into modern self-consistent field (SCF) procedures used to solve Hartree–Fock equations. This makes the theory more comfortable to quantum chemists as well as allowing for the large body of knowledge on the solution of the SCF equations to be used in improving the convergence and efficiency of DFT calculations.

Since the integrals that arise from the formulation of the exchange-correlation functionals in KS-DFT

are of such a complicated nature, numerical quadrature provides the best means for solving them. Most popular quantum chemistry packages, including Q-Chem 2.1, use an atom centered grid procedure recommended by Becke [1]. In this procedure the number of grid points per atom are fixed, and therefore the number of grid points for the total procedure scales linearly with respect to system size. At each grid point though, the amount of work done scales as the number of basis functions squared. To induce linear-scaling, the spatial locality of the density matrix is used to help neglect basis function pairs, so that at some large size, there is effectively a constant amount work to do at each grid point.

Any enhancements to the integration procedure that can accelerate the negation of basis function pairs at each grid point should reduce the prefactor, which will both improve the overall efficiency of the KS-DFT procedure and drop the threshold of system size to achieve linear-scaling. Borrowing from a technique commonly used in SCF procedures, we utilize the difference values in this endeavor. More exactly, we will employ the difference density and functional derivative values, which in turn will make cutoff procedures immensely more effective as the calculation approaches

---

[*] Corresponding author.
  E-mail address: stbrown@psc.edu (S.T. Brown).
[1] Current address: Pittsburgh Supercomputing Centery, Carnegie Mellon University, Pittsburgh, PA 15239, USA.

convergence. Others have preceded this work with similar implementations, including Mitin et al. [2] and Scheiner et al. [3]. We term this technique the Inc-DFT method. In this Letter we show how it can be achieved in a proper mathematical form for KS-DFT energy calculations and discuss the implementational details with analysis of the algorithms performance. We will also outline a variable threshold scheme and show that there is no accumulated error associated with its use in numerical DFT quadrature.

2. Theory and implementation

2.1. Kohn–Sham DFT

In order to outline our implementation, it is necessary to review the well-known formulation of KS-DFT in a finite basis set [4]. The total energy of a molecule can be described by DFT as a functional of the electron density (ρ):

$$E[\rho] = h[\rho] + J[\rho] + E^{XC}[\rho], \tag{1}$$

where h is the one-electron energy contribution, J is the classical Coulomb interaction energy, and E^{XC} is the so-called exchange-correlation energy functional. In the formulation of KS-DFT, h and J are for the Slater determinant that describes a non-interacting reference system, and therefore, they are mathematically equivalent to their counter parts in Hartree–Fock (HF) theory. The crux of this method is the evaluation of the E^{XC} functional by solution of the following integral:

$$E^{XC} = \int f(\rho_\alpha, \rho_\beta, \gamma_{\alpha\alpha}, \gamma_{\beta\beta}, \gamma_{\alpha\beta}) \, d\mathbf{r}, \tag{2}$$

$$\gamma_{\alpha\alpha} = |\nabla\rho_\alpha|^2, \quad \gamma_{\alpha\beta} = \nabla\rho_\alpha \cdot \nabla\rho_\beta. \tag{3}$$

Because the exact form the E^{XC} is unknown, approximate functionals of the electron density (ρ) and its gradient ($\nabla\rho$) attempt to mimic the exchange and correlation hole functions contained in the integral from Eq. (2) [5].

In KS-DFT, the total energy is expressed in a finite basis and is minimized in a self-consistent manner similar to HF theory. In the finite basis, the electron density and its gradients are:

$$\rho_\alpha(\mathbf{r}) = \sum_{\mu\nu} P^\alpha_{\mu\nu} \phi_\mu(\mathbf{r}) \phi_\nu(\mathbf{r}), \tag{4}$$

$$\nabla\rho_\alpha(\mathbf{r}) = \sum_{\mu\nu} P^\alpha_{\mu\nu} \nabla(\phi_\mu(\mathbf{r}) \phi_\nu(\mathbf{r})), \tag{5}$$

where $P^\alpha_{\mu\nu}$ are elements of the α spin density matrix, and similar equations can be formed for ρ_β. An exchange-correlation analogue to the well-known Fock matrix elements from HF theory are given by:

$$F^{XC\alpha}_{\mu\nu} = \int \left[\frac{\partial f}{\partial \rho_\alpha} \phi_\mu \phi_\nu + \left(2\frac{\partial f}{\partial \gamma_{\alpha\alpha}} \nabla\rho_\alpha + \frac{\partial f}{\partial \gamma_{\alpha\beta}} \nabla\rho_\beta \right) \right.$$
$$\left. \cdot \nabla(\phi_\mu \phi_\nu) \right] d\mathbf{r}, \tag{6}$$

with $F^{XC\beta}_{\mu\nu}$ having a similar form.

Generally, the form of the exchange-correlation functional is of such a complicated nature that analytic solutions for the integrals that arise from Eqs. (2) and (6) become impossible. Various numerical techniques have been developed, with the most widely used being proposed by Becke involving a partitioning of the molecular integrals to those solved over atomic centered grids with appropriate weighting functions [1]. The integrals over the atomic grids are evaluated with Euler–Maclaurin [6] quadrature for the radial part and quadrature over Levedev spheres [7–10] for the angular part.

For our work, the extremely efficient implementation of KS-DFT given in Q-Chem 2.1 will be used. Q-Chem 2.1 is a state-of-the-art quantum chemistry suite with a wide-array of computational methods available [11]. Q-Chem includes a robust set of KS-DFT features including: local and gradient corrected functionals; pure and hybrid functionals; analytic energy, gradient and second-derivative evaluations; linear-scaling and parallel algorithms [12,13]; and time-dependent DFT excited state capabilities. Improvements will be made strictly to the numerical engine used for the solution of the exchange-correlation terms of the above equations with plans to apply the IncDFT method to gradient and second derivative calculations. A basic outline of the algorithm for KS-DFT Fock matrix formation in Q-Chem along with the cost associated with each step is provided in Table 1. Each step has a linear dependence on the number of grid points in the molecular grid. It is important to note, that due to the spatial locality of the electron density, the overall scaling of this algorithm can be made linear with respect to the number of grid points for large molecules by effectively making constant the number of close basis functions at each point. Two steps have a square dependence on the number of basis functions and they are the computation of the density values

Table 1
Outline of the basic algorithm for determining the KS-DFT Fock matrix elements in Q-Chem and how each step scales with respect to the number of grid points (N_g) and the number of basis functions (N_b)

Description	Cost
1. Construct the atom centered grid and Becke weighting functions	$O(N_g)$
2. Loop over batches of grid points	
a. Calculate basis function values at each grid point	$O(N_g N_b)$
b. Calculate density values at each grid point	$O(N_g N_b^2)$
c. Calculate functional values at each grid point	$O(N_g)$
d. Sum up contributions to Fock Matrix element	$O(N_g N_b^2)$
End loop over-batchs of grid points	

on the grid (Step 2b in Table 1) and the summation of each Fock Matrix element (Step 2d in Table 1). In trying to improve the efficiency of our KS-DFT algorithm, these two rate-limiting steps are targeted. The easiest method for improving this algorithm is to screen insignificant values for elimination from the summations, and IncDFT can be utilized to improve the screening effectiveness.

2.2. IncDFT

IncDFT is a method that utilizes the iterative nature of the KS-DFT procedure to increase the effectiveness of screening values. Suppose that at each iteration, a quantity f is calculated as a function of the variable x, where $f(x)$ is linear in x. Instead of calculating f directly from each new x, it is possible to determine f as the variable difference between x at the current cycle and at the previous cycle (x^{prev}):

$$f(x) = f(\Delta x) + f^{\mathrm{prev}}, \quad \Delta x \equiv x - x^{\mathrm{prev}}. \tag{7}$$

As the iterative procedure progresses, it will be true that Δx will become increasingly smaller which in turn allows the elimination from consideration the current values with insignificant change from the previous iteration. This concept is utilized to accelerate HF calculations in the form of the incremental Fock formation [14–17].

At first glance, Eq. (7) is not immediately applicable to the numerical evaluation of the KS-DFT integrals for the current widely used exchange correlation functionals are not linear with respect to the electron density. The equation is however applicable to portions of the algorithm that do not involve non-linear functions of the density, namely the evaluation of density values on the grid (Step 2b in Table 1) and the Fock matrix formation (Step 2d in Table 1). With this in mind, we propose a new algorithm for KS-DFT in Table 2, which we have termed IncDFT. In the new algorithm, values from the previous iteration are stored in order to use in producing

difference values. To keep the algorithm mathematically correct, the difference density values that are computed on the grid (Step 4b in Table 2) are combined with the values from the previous iterations (Step 4c in Table 2) to reproduce the current values from the current iteration. Then the full non-difference values are used as the functional variable (Step 4e in Table 2) and therefore circumventing any problems with non-linear functional evaluation. The functional derivative values from the previous iteration can be subtracted from the current to create difference values for use in the Fock matrix formation (Steps 4f–h in Table 2).

In the IncDFT scheme, we must derive new expressions for the density and gradient of the density on the grid. This is trivially done by incorporating Eq. (7) into Eqs. (4) and (5):

$$\rho_\alpha(\mathbf{r}_g) = \sum_{\mu\nu} \Delta P^\alpha_{\mu\nu} \phi_\mu(\mathbf{r}_g)\phi_\nu(\mathbf{r}_g) + \rho^{\mathrm{prev}}_\alpha(\mathbf{r}_g), \tag{8}$$

$$\nabla\rho_\alpha(\mathbf{r}_g) = \sum_{\mu\nu} \Delta P^\alpha_{\mu\nu} \nabla(\phi_\mu(\mathbf{r}_g)\phi_\nu(\mathbf{r}_g)) + \nabla\rho^{\mathrm{prev}}_\alpha(\mathbf{r}_g), \tag{9}$$

where the superscript prev stands for the corresponding value from the previous iteration and the subscript g denotes the current grid point. Much like the incremental Fock method, this formula takes advantage of the observation that a large number of the elements of the density matrix change very little between two consecutive iterations, especially near convergence. Screening against a threshold can then be done on the density matrix elements $P_{\mu\nu}$ and $\mu\nu$ shell pairs can be eliminated from further consideration. Some preliminary computations applying Eq. (8) indicated that the value $\Delta P_{\mu\nu}\|\phi_\mu\phi_\nu\|$, where $\|\phi_\mu\phi_\nu\|$ is an estimation the magnitude of the shell pair [16,17], is far more productive as a screening value in that it is more representative of the true values being screened from Eq. (8). For gradient corrected functionals, an estimation of the magnitude of the gradient of the shell pair is given by scaling $\|\phi_\mu\phi_\nu\|$

Table 2
Outline of the IncDFT algorithm for determining the KS-DFT Fock matrix elements in Q-Chem and how the computational work and storage requirements scale with respect to the number of grid points (N_g) and the number of basis functions (N_b)

Description	Cost	Storage
1. Construct the atom centered grid and Becke weighting functions	$O(N_g)$	
2. Compute and screen the difference density matrix $\Delta P_{\mu\nu}$	$O(N_b^2)$	
3. Store the density matrix from the current iteration	$O(N_b^2)$	$O(N_b^2)$
4. Loop over batches of grid points		
a. Calculate basis function values at each grid point, $\phi_\mu(r_g)$	$O(N_g N_b)$	
b. Calculate difference density values at each grid point	$O(N_g N_b^2)$	
c. Add the density values from the previous iteration to the difference values to get current values	$O(N_g)$	
d. Store the current density values	$O(N_g)$	$O(N_g)$
e. Calculate functional values at each grid point	$O(N_g)$	
f. Compute and screen the difference functional derviative values, Δf	$O(N_g)$	
g. Store the current functional derivative values	$O(N_g)$	$O(N_g)$
h. Sum up contributions to Fock matrix element	$O(N_g N_b^2)$	
End loop over batches of grid points		

with the sum of the individual shell exponents. This screening will result in an overall reduction in the number of basis function pairs that need to be considered.

For the summations of values to form Fock matrix elements, the difference of functional derivative values, $\Delta f'(\rho(r_g))$, are used. For pure functionals, the derivation from Eq. (6) is trivial. Beginning here, an abbreviated notation will be used to simplify the formulas. Functional derivatives will denoted with a superscript giving the variable with which respect the derivative was taken (e.g. $f^{\rho_\alpha} = \partial f / \partial \rho_\alpha$).

$$F_{\mu\nu}^{XC\alpha} = \sum_g w_g \Delta f_g^{\rho_\alpha} \phi_{\mu,g} \phi_{\nu,g} + F_{\mu\nu}^{XC\alpha \ prev}, \tag{10}$$

where the subscript g denotes the value at a grid point. The screened value in this case is naturally $w_g \Delta f_g^{\rho_\alpha}$ and small values will eliminate grid points from further consideration. Once again, preliminary calculations indicated that screening this value alone would not be adequate. To improve screening, the above value is multiplied by the square of the maximum basis function value for the given grid point, which yields the maximum contribution that is made to Eq. (10) by that point.

Gradient corrected functionals make for a more complicated IncDFT framework. The α Fock matrix elements are:

$$F_{\mu\nu}^{XC\alpha} = \sum_g w_g f_g^{\rho_\alpha} \phi_{\mu,g} \phi_{\nu,g} + w_g (2 f_g^{\gamma_{\alpha\alpha}} \nabla \rho_{\alpha,g} + f_g^{\gamma_{\alpha\beta}} \nabla \rho_{\beta,g})$$
$$\cdot \nabla(\phi_{\mu,g} \phi_{\nu,g}). \tag{11}$$

The difference between interaction cycles for the alpha Fock matrix elements can be expressed as:

$$\Delta F_{\mu\nu}^{XC\alpha} = \sum_g w_g \Delta f_g^{\rho_\alpha} \phi_{\mu,g} \phi_{\nu,g}$$
$$+ w_g \Delta(2 f_g^{\gamma_{\alpha\alpha}} \nabla \rho_{\alpha,g} + f_g^{\gamma_{\alpha\beta}} \nabla \rho_{\beta,g}) \cdot \nabla(\phi_{\mu,g} \phi_{\nu,g}). \tag{12}$$

The difference variable in the second term of the summation must be $\Delta(2 f_g^{\gamma_{\alpha\alpha}} \nabla \rho_{\alpha,g} + f_g^{\gamma_{\alpha\beta}} \nabla \rho_{\beta,g})$ because the gradients of the density and the functional derivative values change between iterations. Along with $\Delta f_g^{\rho_\alpha}$ these are the values that should be screened. The square of the maximum value of the gradient of the density at each grid point will be multiplied by the latter for more effective screening as proposed above. A grid point will only be eliminated if both of the screening values are below thresholds.

In the spin unrestricted formalisms, consideration needs to be given to both alpha and beta densities, so there are two sets of corresponding values to screen. In a closed-shell case, there would be no difference in the amount of values neglected, but this is not so for open-shell calculations. It would potentially be more advantageous to screen each spin density separately, although one would need to double many of the mem-

ory requirements. Based on some preliminary calculations, it was apparent that the savings were minuscule and did not justify the extra memory. So, in our unrestricted scheme, the values are neglected only if both α and β values are below threshold.

It is important that any efficiency improvements to the current KS-DFT scheme not increase the scaling of the algorithm with respect to both memory and computations. In order to have available the values from previous iterations, it is necessary to store in memory or on disk several quantities. Table 2 shows the values that need be stored and the scaling of storage. It is true that storage of the previous cycle's density matrix scales as square of the number of basis functions, but it is already necessary to store the current cycle's density matrix, so this does not effectively increase the overall storage scaling for the algorithm. The other two quantities to be stored scale linearly with the number of grid points. In Table 2, we see the computational scaling for the added steps do not increase the overall computational scaling of the algorithm, as the rate-limiting steps, the computation of density values and the summation to form Fock matrix elements, still scale as the number of grid points and the square of the number of basis functions, although the number of basis function pairs considered should be greatly reduced.

2.3. Variable threshold method

A common method for increasing the efficiency of iterative procedures is to employ some form of variable threshold determined from the error of the previous iteration. The hope is that the error at early iterations will not be as critical to convergence as in the later cycles and the threshold to neglect values can be reduced in some prescribed manner as the calculation proceeds. This allows the algorithm to neglect more values at the beginning of the procedure without significantly sacrificing the overall accuracy of the final result.

The use of a variable threshold can yield impressive increases in efficiency. Furthermore, unlike HF theory, the variable threshold in IncDFT is proper as the error does not accumulate with each progressive iteration, as long as the values for the previous iteration are used if the current difference is omitted. In HF theory, the error does accumulate and has a $\sqrt{n_{\text{iteration}}}$ dependence [14,17]. To illustrate this point, let us assume that a calculation takes four iterations to converge. The density value at a grid point for the final iteration can always be evaluated cumulatively:

$$\rho_4 \equiv (\rho_4 - \rho_3) + (\rho_3 - \rho_2) + (\rho_2 - \rho_1) + \rho_1. \tag{13}$$

If a difference is omitted, e.g. $(\rho_3 - \rho_2)$, because it is smaller than the current threshold, it does not impose any approximation if ρ_3 is assumed to be equal to ρ_2:

$$\rho_4 \equiv (\rho_4 - \rho_2) + (\rho_2 - \rho_1) + \rho_1. \tag{14}$$

The analogous argument can be made for the difference funcitonal derivative values used in the formation of the Fock matrix.

While this speaks to the accumulation of error, it does not preclude that the absolute error at each iteration will not affect the convergence, so it must be ensured that the method for determining the threshold at each iteration provides accurate results. It is known that poorly chosen variable thresholds can cause undesirable convergence behavior [14,18]. In order to address this, we looked at the threshold as a function of the error in the approximate values produced at each iteration of the calculation in comparison to exact values for AZT with the Becke exchange functional [19] and the LYP correlation functional [20]. It is found that setting the variable threshold to the energy at the previous iteration scaled by 1×10^{-4} gives maximum errors that are on the order of or lower than the current iteration's error (in the case of Q-Chem, this is the error from the direct inversion of the iterative subspace (DIIS) procedure as described by Pulay [21]). This is the scheme we have adopted in all following results that state variable threshold is used.

3. Results and discussion

3.1. AZT

In order to effectively display the benefits gained from the IncDFT procedure, extensive analysis of the various parts of the algorithm were probed using 3′-azido-3′-deoxythymidine (AZT) as a benchmark. AZT is a widely used antiretroviral agent against the HIV-1 virus [22]. The 6-31G basis set is used in conjunction with the Becke exchange functional [19] and the LYP correlation functional [20]. The AZT molecule has 32 atoms and the calculations consists of 311 basis functions. All of our calculations will be spin-restricted computations, although it is important to note that the algorithm has been extended to the unrestricted formalism. The self-consistent KS-DFT procedure was considered converged once the DIIS error was less than 10^{-5}. For these test calculations, three 'static' thresholds, 10^{-6}, 10^{-8}, 10^{-10}, and the variable threshold as described in the previous section were used. All of these thresholds are tighter than the convergence criteria and should give an good indication of performance and accuracy of the IncDFT procedure. All calculations in this section were performed on an IBM RS/6000 260.

The most desirable aspect of IncDFT is that as the self-consistent calculation approaches convergence, more values will be screened than in previous iterations. Figs. 1 and 2 display graphs of the percentage of values saved in the time consuming steps at each iteration. For all of the 'static' thresholds, there is a definite increase in the percentage of values screened as the calculation approaches convergence and as the threshold is decreased the screening become less pronounced. In both procedures, setting the threshold to 10^{-6} gives the most savings for the later stages, even neglecting almost the entire grid for the final iteration of the Fock formation procedure. The variable threshold performs very well throughout the entire calculation, giving savings falling between that of 10^{-6} and the 10^{-8} thresholds. The reason for the similar performance is that the overall threshold for the KS-DFT procedure in Q-Chem for a convergence criteria of 10^{-5} is set to 10^{-8}, so once the variable threshold reached that value, it was held constant. The 10^{-10} shows that increasing this value beyond the overall integration threshold gives little savings.

Enhancing the screening process has the potential for increasing the approximate nature of the numerical integration, so it is important to test the algorithm to ensure that the accuracy of the original procedure is preserved. Tables 3 and 4 show the absolute total energy difference
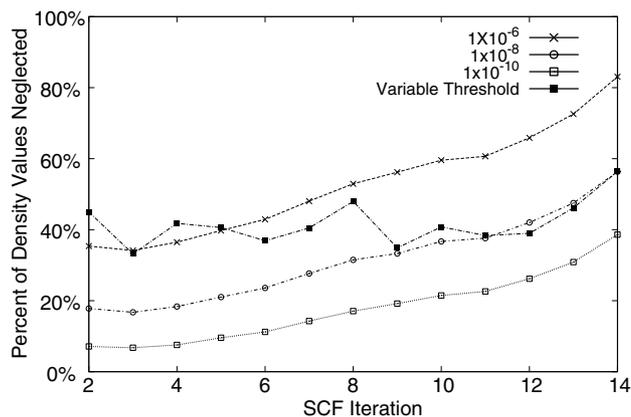

Fig. 1. The percentage of density values screened out of the BLYP/6-31G AZT calculation at each iteration of the SCF procedure.
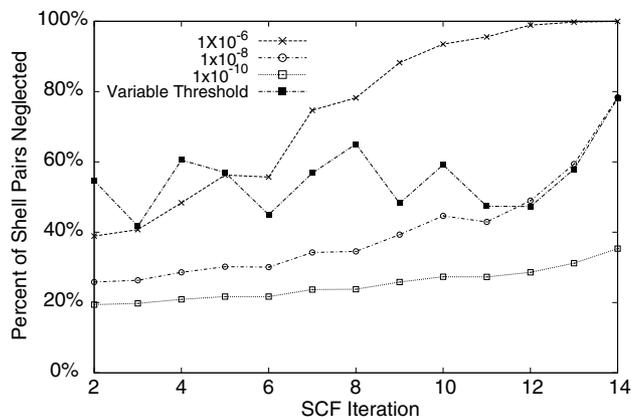

Fig. 2. The percentage of shell pairs neglected as a result of screening the difference functional derivative values for BLYP/6-31G AZT at each SCF iteration.

Table 3
Absolute difference in the BLYP/6-31G total energy (hartrees) of AZT for each iteration between the original numerical integration algorithm and IncDFT with various thresholds for screening the density values in Step 4b of Table 2

Iteration[a]	DIIS error	Log of the IncDFT threshold			
		6	8	10	Variable[b]
2	$1.07E-02$	$6.1e-05$	$1.8e-06$	$2.9e-09$	$1.3e-03$
3	$2.90E-02$	$4.9e-05$	$2.2e-06$	$8.7e-09$	$7.2e-06$
4	$1.40E-02$	$1.6e-05$	$2.0e-06$	$1.0e-09$	$4.1e-04$
5	$5.23E-03$	$5.5e-05$	$4.2e-06$	$5.6e-09$	$2.1e-04$
6	$3.33E-03$	$7.8e-05$	$2.7e-06$	$2.0e-09$	$2.1e-05$
7	$4.13E-03$	$1.3e-04$	$3.0e-06$	$4.7e-09$	$6.1e-05$
8	$8.73E-04$	$2.9e-04$	$2.4e-06$	$1.3e-08$	$2.4e-05$
9	$4.96E-04$	$1.8e-04$	$1.2e-06$	$9.8e-09$	$3.7e-06$
10	$2.58E-04$	$1.9e-04$	$5.9e-08$	$1.9e-09$	$2.8e-06$
11	$1.26E-04$	$1.3e-04$	$2.4e-06$	$1.4e-08$	$6.8e-06$
12	$5.70E-05$	$1.4e-04$	$4.9e-07$	$5.2e-09$	$7.4e-07$
13	$1.95E-05$	$1.9e-04$	$1.8e-06$	$9.2e-09$	$2.1e-06$
14	$7.89E-06$	$1.4e-04$	$1.9e-06$	$9.2e-09$	$2.2e-06$

The calculation was continued until the DIIS difference reached a convergence of 10^{-5}.
[a] The first iteration is omitted because there is no difference between the algorithms.
[b] The variable threshold is as defined in Section 2.3 of this Letter.

in hartrees between the IncDFT algorithm and the original at various thresholds along with the DIIS error at each iteration for the benchmark calculation. Just as above, each calculation was until the DIIS reached a convergence of 10^{-5}, and the 'static' thresholds were chosen to be 10^{-6}, 10^{-8} and 10^{-10}. Also the so-called variable threshold results are available.

In Table 3, the differences are given for the screening of the density values. It is apparent that error control is possible for the density evaluation, for the energy difference gets smaller as the threshold is lowered. A threshold of 10^{-6} appears to be too loose a value for the final difference in the energy is actually higher than the DIIS error of the final iteration, and the threshold must be tightened to 10^{-8} to ensure that the final iterations are at least on the order of the DIIS error. The variable

threshold yields similar final errors as using 10^{-8}, which is expected since it is made constant once it reaches that value. Table 4 shows the differences arising from IncDFT screening of the difference functional derivative values, and similar trends can be seen. It appears that accuracy of the method is less sensitive than in the case of screening density values, and only a value of 10^{-6} is necessary to be on the order of the DIIS error. The variable threshold performs similarly as in the case of the screening of the density values. In both cases, increasing the value of the thresholds beyond the overall integral threshold, as in 10^{-10}, is unnecessary to provide reliable accuracy.

Finally, it is imperative that the IncDFT procedure adds no significant overhead to the existing algorithm. As discussed in the previous section, none of the

Table 4
Absolute difference in the BLYP/6-31G total energy (hartrees) of AZT for each iteration between the original numerical integration algorithm and IncDFT with various thresholds for screening the difference functional derivative values in forming XC Fock matrix values in Step 4f of Table 2

Iteration[a]	DIIS error	Log of the IncDFT threshold			
		6	8	10	Variable[b]
3	$2.90E-02$	$2.4e-03$	$3.5e-05$	$4.7e-06$	$2.0e-02$
4	$1.40E-02$	$6.6e-05$	$6.3e-06$	$3.0e-07$	$5.2e-03$
5	$5.23E-03$	$9.6e-05$	$1.1e-06$	$1.0e-07$	$1.4e-03$
6	$3.33E-03$	$1.2e-04$	$5.4e-07$	$3.7e-08$	$3.9e-05$
7	$4.13E-03$	$9.4e-05$	$2.8e-06$	$3.5e-08$	$1.3e-04$
8	$8.73E-04$	$1.8e-05$	$9.7e-08$	$3.0e-08$	$1.4e-04$
9	$4.96E-04$	$7.8e-07$	$1.9e-07$	$1.5e-08$	$5.6e-05$
10	$2.58E-04$	$4.8e-07$	$2.9e-08$	$3.7e-09$	$1.2e-05$
11	$1.26E-04$	$1.5e-05$	$5.1e-09$	$1.5e-09$	$3.1e-06$
12	$5.70E-05$	$3.7e-06$	$1.0e-08$	$3.6e-09$	$3.7e-07$
13	$1.95E-05$	$3.3e-06$	$1.1e-08$	$3.7e-09$	$6.9e-08$
14	$7.89E-06$	$3.2e-06$	$5.6e-09$	$6.7e-09$	$8.9e-08$

The calculation was continued until the DIIS difference reached a convergence of 10^{-5}.
[a] The first and second iteration in omitted because there is no difference between the algorithms.
[b] The variable threshold is as defined in Section 2.3 of this Letter.

additional steps for IncDFT increased the overall scaling of computation. Figs. 3 and 4 are graphs of the percentage of values neglected by IncDFT screening with respect to the percentage of time saved in the procedure due to the screening. If there is no increase in scaling, it would be expected that there would be essentially a linear relationship between these two percentages, and in both cases, this is true.

In both cases, when 100% of the values are neglected there is a non-zero time for performing the algorithm, and this is the overhead associated with doing IncDFT. This overhead amounts to approximately 5% and 3% for the density evaluation and the Fock matrix formation, respectively. Also there are parts within these algorithms that do not benefit from IncDFT procedure. To illus-

trate this, Figs. 3 and 4 also contain plots of the most time consuming steps involved in the computation of values. For determining the density values on the grid, the contraction of the basis function pairs and gradients with the density matrix elements is the limiting step. It can be seen that the slope of the line associated with the total percentage of time to compute the values is less than that for the contraction step which is an indication that there other significant parts that do not benefit from IncDFT, but it is apparent that the time savings in the contraction step dominates. In the building of Fock matrix elements the time-consuming step is the contraction of the basis function pairs with the functional derivatives. Unlike the previous case, Fig. 4. shows that basically in the overall algorithm the contraction step dominates and IncDFT is equally beneficial. The fact that the time-consuming steps dominate as expected vindicates the slight overhead involved in the IncDFT procedure and shows great improvements in efficiency can be reached.

Table 5 shows the overall percentage savings from the IncDFT procedure for the benchmark AZT 6-31G/BLYP calculation with the variable threshold. The savings achieved from the improved screening translates well to overall time savings in the time consuming steps, with 31% and 48% savings in computing density value on the grid and the formation of the Fock matrix elements respectively (see Table 6).
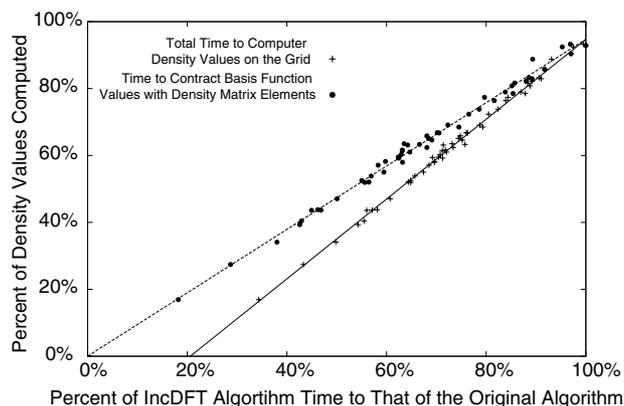

Fig. 3. The percentage of density values screened plotted against the percentage of time saved in the evaluation of the density on the grid for BLYP/6-31G AZT. Shown are the total times for the procedure and just the step involving contraction of the basis function pairs with the density matrix elemtents. The slope for the total time and the contraction step are 1.2 and 0.95, respectively.
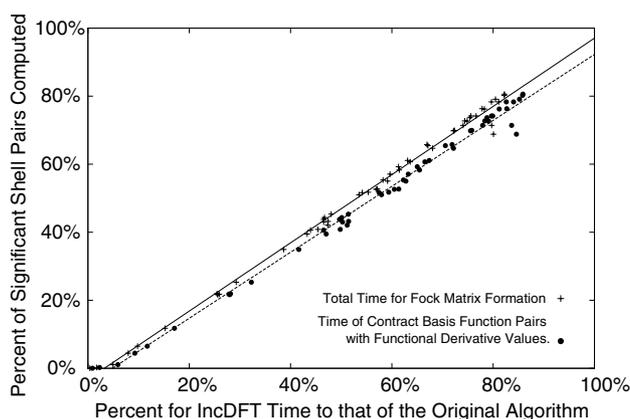
3.2. Other examples

To show the applicability of the IncDFT method, Table 5 shows the increase in the overall efficiency of determining the KS-DFT energy with various functionals for several different molecules. The best overall savings in integration time by application of the method to the EDF1/6-31G* calculation on the Buckminster fullerene (C_{60}), in which there is approximately a 45% increase in efficiency.

Fig. 4. The percentage of density values screened plotted against the percentage of time saved in the evaluation of the F^{XC} matrix elements for BLYP/6-31G AZT. Shown are the total time for the procedure and just the step involving contraction of the basis function pairs with the functional derivative values. The slope for the total time and the contraction step are 0.99 and 1.00, respectively.

Table 5
Percentage of total savings from the the variable threshold IncDFT procedure for the BLYP/6-31G AZT single-point energy calculation

Determination of the density values on the grid	
Number of density matrix neglected	39%
Number of basis function pairs neglected	42%
Savings in time for the contraction with basis function pairs	39%
Savings in total time	31%
Formation of the Fock matrix elements	
Number of grid points neglected	46%
Number of basis function pairs neglected	55%
Savings in time for the contractions of basis function pairs	51%
Savings of total time	48%

Table 6
Percentage of savings from the the variable threshold IncDFT procedure in the overall DFT integration procedure with various functionals and basis sets for several molecules

Molecule	Functional	Basis set	Percent savings
Glutamine (20 atoms)	B3LYP	6-31G (160 functions)	20%
Tryptophan (27 atoms)	BPW91	6-31G* (249 functions)	23%
Taxol (113 atoms)	BLYP	6-3 1G* (1032 functions)	35%
C_{60} Buckminster Fullerine (60 atoms)	EDF1	6-31G* (900 functions)	45%

4. Concluding remarks

The IncDFT method has been shown to be an effective means of improving the efficiency of the KS-DFT integration procedure. As shown in the case of 6-31G/BLYP AZT, significant overhead is not incurred through use of the method and the savings in the most time consuming steps certainly justify its use. The variable threshold is shown here to provide a good balance between improving efficiency and maintaining the accuracy of the integration procedure and is the recommended cutoff scheme for use in production. In the case of larger molecules, such as taxol and the Buckminster fullerene, IncDFT with the variable threshold yields a 35%–45% improvement.

Acknowledgments

References

[1] A.D. Becke, J. Chem. Phys. 88 (1988) 2547.
[2] A.V. Mitin, J. Baker, K. Wolinski, P. Pulay, J. Comput. Chem. 24 (2002) 154.
[3] A.C. Scheiner, J. Baker, J.W. Andzelm, J. Comput. Chem. 18 (1997) 775.
[4] P.M.W. Gill, B.G. Johnson, J.A. Pople, Chem. Phys. Lett. 209 (1993) 506.
[5] B.G. Johnson, P.M.W. Gill, J.A. Pople, J. Chem. Phys. 98 (1993) 5612.
[6] C.W. Murray, N.C. Handy, G.J. Laming, Mol. Phys. 4 (1993) 997.
[7] V.I. Lebedev, Z. Vychisl, Mat. Mat. Fiz. 15 (1975) 48.
[8] V.I. Lebedev, Z. Vychisl, Mat. Mat. Fiz. 16 (1976) 293.
[9] V.I. Lebedev, Sib. Mat. Zh. 18 (1977) 132.
[10] V.I. Lebedev, A.L. Skorokhodov, Russ. Acad. Sci. Dokl. Math. 45 (1992) 587.
[11] J. Kong, C.A. White, A.I. Krylov, C.D. Sherrill, R.D. Adamson, T.R. Furlani, M.S. Lee, A.M. Lee, S.R. Gwaltney, T.R. Adams, et al., J. Comput. Chem. 21 (2000) 1532.
[12] P.P. Korambath, J. Kong, T.R. Furlani, M. Head-Gordon, Mol. Phys. 100 (2002) 1755.
[13] T. Furlani, J. Kong, P.M.W. Gill, Comp. Phys. Commun. 128 (2000) 170.
[14] E. Schwegler, M. Challacombe, M. Head-Gordon, J. Chem. Phys. 106 (1997) 9708.
[15] J. Almlöf, K. Faegri, K. Korsell, J. Comp. Chem. 3 (1982) 385.
[16] D. Cremer, J. Gauss, J. Comp. Chem. 7 (1986) 274.
[17] M. Häser, R. Ahlrichs, J. Comp. Chem. 10 (1989) 104.
[18] G.E. Scuseria, J. Phys. Chem. 103 (1999) 4782.
[19] A.D. Becke, Phys. Rev. A 38 (1988) 3098.
[20] C. Lee, W. Yang, R.G. Parr, Phys. Rev. B 37 (1988) 785.
[21] P. Pulay, Chem. Phys. Lett. 73 (1980) 393.
[22] L. Menéndez-Arias, T. Pharm. Sci. 23 (2002) 381.